temperature, 120 K. Therefore, we conclude that the formation of the 2D small polaron is governed by quantum dissipative processes such as tunneling, and the classical theory is not applicable to this system.

It is encouraging that the parameters extracted from the fit (legend to Fig. 5A) are consistent with known values for polarons in other molecular solids: E_{rc} is consistent with the dynamic modulation of the polarization energy (~0.03 eV) for electron-phonon interaction in organic crystals, and E_{rq} is similar to the effective formation energy (0.15 eV) of a molecular polaron in polyacene crystals (*23*). The lattice relaxation energy ($E_{rel} = E_{rc} + E_{rq}$) is comparable to the localization energy E_{loc} (*24*), and hence, the self-trapping energy (Eq. 3) is small for this system. The energy of $\hbar\omega_q$ corresponds to an in-phase methylene rocking mode of *n*-heptane (*25*). The oscillatory dependence of k_{st} on $-\Delta\varepsilon$ (Fig. 5A) is reproduced. The first maximum corresponds to the usual classical inverted region resulting from the intermolecular modes ($-\Delta\varepsilon = E_{rc}$). Subsequent maxima originate from a resonant effect resulting from the excitation of the intramolecular mode (*26*) and the interval between maxima is $\hbar\omega_q$ (see Fig. 5A). Finally, with the use of the above parameters and path integral theory, the temperature dependence of k_{st} is reproduced with no other adjustable parameters (Fig. 5B). The non-Arrhenius behavior results from nuclear tunneling in the high-frequency mode.

Our results demonstrate that the ability to both time- and angle-resolve the dynamics of electrons at interfaces allows a quantitative determination of the relaxation energies and lattice displacements associated with the small-polaron self-trapping process. Our results provide an experimental basis for further theoretical studies. Time- and angle-resolved TPPE is a powerful probe for 2D electron localization and should also be applicable to a wide variety of interfaces.

REFERENCES AND NOTES

1. For reviews, see A. L. Shluger and A. M. Stoneham, *J. Phys. Condens. Matter* **5**, 3049 (1993); K. S. Song and R. T. Williams, *Self-Trapped Excitons* (Springer-Verlag, Berlin, 1993).
2. L. D. Landau, *Phys. Z. Sowjetunion* **3**, 664 (1933); E. I. Rashba, *Opt. Spektrosk.* **2**, 75 (1957); Y. Toyozawa, *Prog. Theor. Phys.* **26**, 29 (1961).
3. W. Hayes and A. M. Stoneham, *Defects and Defect Processes in Nonmetallic Solids* (Wiley, New York, 1985).
4. A. R. Burns, E. B. Stechel, D. R. Jennison, Eds., *Desorption Induced by Electronic Transitions* (Springer-Verlag, Berlin, 1993).
5. J. G. Bednorz and K. A. Muller, *Z. Phys. B* **64**, 189 (1986); D. Mihailovic *et al.*, Eds. *Anharmonic Properties of High-Tc Cuprates* (World Scientific, Singapore, 1995).
6. K. Giesen, F. Hage, F. J. Himpsel, H. J. Riess, W. Steinmann, *Phys. Rev. Lett.* **55**, 300 (1985). For a review, see Th. Fauster and W. Steinmann, in *Photonic Probes of Surfaces*, P. Halevi, Ed. (Elsevier, Amsterdam, 1995), pp. 347–411. For a study of coherence phenomena, see U. Höfer *et al.*, *Science* **277**, 1480 (1997).
7. P. M. Echenique and J. B. Pendry, *Prog. Surf. Sci.* **32**, 111 (1990).
8. D. F. Padowitz, W. R. Merry, R. E. Jordan, C. B. Harris, *Phys. Rev. Lett.* **69**, 3583 (1992).
9. R. L. Lingle Jr., N.-H. Ge, R. E. Jordan, J. D. McNeill, C. B. Harris, *Chem. Phys.* **205**, 191 (1996); *ibid.* **208**, 297 (1996).
10. R. L. Lingle Jr., D. F. Padowitz, R. E. Jordan, J. D. McNeill, C. B. Harris, *Phys. Rev. Lett.* **72**, 2243 (1994). In that paper, both localized and delocalized state appeared to coexist when studied with 6-ps time resolution.
11. Y. Toyozawa, in *Relaxation of Elementary Excitations*, R. Kubo and E. Hanamura, Eds. (Springer-Verlag, Berlin, 1980), pp. 3–18; A. J. Fisher, W. Hayes, D. S. Wallace, *J. Phys. Condens. Matter* **1**, 5567 (1989).
12. T. L. Gilbert, *Lecture Notes for NATO Summer School in Solid State Physics*, Ghent, Belgium (1966) [unpublished, referenced in (*1*)].
13. D. Emin and T. Holstein, *Phys. Rev. Lett.* **36**, 323 (1976); Y. Toyozawa and Y. Shinozuka, *J. Phys. Soc. Jpn.* **48**, 472 (1980); H. Sumi, in *Excitonic Processes in Condensed Matter, Proc. SPIE 2362*, J. Singh, Ed. (SPIE, Bellingham, WA, 1995), pp. 108–119.
14. That is, optical excitation primarily promotes electrons from delocalized metal states into delocalized image-potential states without lattice distortion.
15. L. E. Firment and G. A. Somorjai, *J. Chem. Phys.* **69**, 3940 (1978).
16. R. A. Marcus and N. Sutin, *Biochim. Biophys. Acta* **811**, 265 (1985); J. Ulstrup, *Charge Transfer Processes in Condensed Media* (Springer-Verlag, Berlin, 1979).
17. Exothermicity $-\Delta\varepsilon$ is determined by the photoelectron kinetic energy difference between the delocalized and localized states (see Fig. 1, B and C).
18. T. Holstein, *Ann. Phys.* **8**, 325 (1959); *ibid.*, p. 343.
19. R. A. Marcus, *J. Chem. Phys.* **24**, 966 (1956).
20. A. A. Stuchebrukhov and X. Song, *ibid.* **101**, 9354 (1994).
21. In this analysis, we attributed the decay rate of the delocalized state (after subtracting a rate for tunneling back into the metal which is independent of $k_{\parallel}$) to self-trapping. We ignored the possible contribution from intraband relaxation by way of electron-phonon scattering for the following reasons. First, a perturbation calculation of the rate of scattering against 2D acoustic phonons of the alkane layers did not give reasonable agreement with the energy dependence of the decay rate of delocalized states. Second, delocalized states at 50 K decay faster than at 120 K, contradicting the scattering theory prediction. However, scattering may play a role in causing the finite rise time of the delocalized state. It may also be related to the similar dynamics recently observed in the neopentane-Ag(111) system. Further studies are required to address these issues.
22. However, at 50 K, the first-order term accounts for only 83% of the rate.
23. E. A. Silinsh and V. Capek, *Organic Molecular Crystals: Interaction, Localization, and Transport Phenomena* (AIP Press, New York, 1994).
24. Within the isotropic 2D tight-binding approximation, the half width of the delocalized band *B* can be estimated from m^* by $B = 2\hbar^2/m^*a^2$, where *a* is the lattice constant. The measured $m^* = 1.2m_e$ is an average value over *n*-heptane domains grown on the threefold symmetric Ag(111) with domain axes rotated by 120°. For a crude estimate of *B*, we assume a square lattice with the area of *n*-heptane surface mesh (*15*). Therefore, we obtained $E_{loc} \sim 0.25$ eV.
25. R. G. Snyder, *J. Chem. Phys.* **47**, 1316 (1967).
26. S. Efrima and M. Bixon, *Chem. Phys.* **13**, 447 (1976).

27. We thank X. Song for helpful discussions. Supported by the Director, Office of Energy Research, Office of Basic Energy Sciences, Chemical Sciences Division of the U.S. Department of Energy, under contract DE-AC03-76SF00098. Specialized equipment used in some experiments described herein was supported by NSF.

21 August 1997; accepted 3 November 1997

Photonic Channels for Quantum Communication

S. J. van Enk, J. I. Cirac, P. Zoller

A general photonic channel for quantum communication is defined. By means of local quantum computing with a few auxiliary atoms, this channel can be reduced to one with effectively less noise. A scheme based on quantum interference is proposed that iteratively improves the fidelity of distant entangled particles.

Security for communication of sensitive data over public channels such as the Internet is indispensable nowadays. Quantum mechanics offers the possibility of storing, processing, and distributing information in a proven secure way by exploiting the fragility of quantum states and the fact that they cannot be cloned (*1*). In practice, many obstacles stand in the way of implementing a reliable quantum network. Although remarkable progress has recently been made experimentally in the context of quantum cryptography and computation (*2*), the presence of errors during the transmission and processing of quantum information remains as the main obstacle. In principle, these problems could be circumvented with ingenious schemes for purifying states (*3*) and correcting errors (*4*), because they allow the transmission of intact quantum states even in the presence of errors. These "standard" methods require a large (in principle, infinite) number of extra quantum bits (qubits) to store intermediate information. However, in the first generations of experiments on quantum networks, one expects to be able to store and manip-

Institut für Theoretische Physik, Universität Innsbruck, Technikerstrasse 25, A-6020 Innsbruck, Austria.

ulate only a few qubits in each location. Thus, new methods are needed to overcome the presence of errors during quantum communication in small physical systems.

Recently we proposed a physical implementation based on cavity quantum electrodynamics (QED) (5) to accomplish ideal transmission over a noisy channel where the dominant error is due to photon absorption (6). We modeled photon absorption by a Markovian process and showed how this property can be exploited to convey intact quantum information within a quantum network composed of small physical systems. Although this assumption is restrictive, it shows that one has to reconsider the definition of quantum channels, which leads to nonstandard methods of purification and error correction.

In this work we define a general channel for communication via photons and show how to transmit quantum information via that channel. This channel is not based on a particular physical model, does not use the Markov property, and includes all possible errors during transmission. Moreover, in contrast to usual definitions of noisy quantum channels [such as the depolarizing channel or the erasure channel (7)], we do not describe the action of the channel only in terms of classical probabilities but allow for quantum interference effects. In fact, these quantum interferences allow one, under certain conditions, to transmit quantum states over channels that have so much noise in terms of classical probabilities that one would be led to believe no quantum information could be transmitted at all. The scheme we propose is based on "channel reduction," which consists of combining local operations and measurements with multiple uses of the channel to reduce the description to a simplified effective channel. Using this effective channel and exploiting quantum interference effects, we show how to create a perfect distant maximally entangled state [Einstein-Podolsky-Rosen (EPR) pair] utilizing only three qubits at each location. With teleportation, one can then send any unknown quantum state securely without distortions (8).

To define the photonic channel, we denote by $|0\rangle$ and $|1\rangle$ the states of the qubit that a sender, traditionally called Alice, transmits to the receiver Bob, and by $|E\rangle$ the initial state of the environment. The action of the most general channel leaving the qubit inside its original two-dimensional (2D) Hilbert space is

$$|0\rangle|E\rangle \mapsto (|0\rangle T_{00} + |1\rangle T_{01})|E\rangle \quad (1a)$$

$$|1\rangle|E\rangle \mapsto (|0\rangle T_{10} + |1\rangle T_{11})|E\rangle \quad (1b)$$

where the operators T act on the environment. In analogy with the definition of classical channels, one typically characterizes a channel by the probability that a qubit is transmitted without distortion, as well as the probability of occurrence of certain specific errors. For example, the depolarizing channel (7) assumes that with probability F the qubit is transmitted intact and with probabilities $(1 - F)/3$ it suffers a sign flip, a spin flip, or both, which are represented by the Pauli spin operators $\sigma_{z,x,y}$ acting on the qubit. One usually has in mind a situation where the states of the qubit correspond to two orthogonal polarizations of a photon. Errors are changes of polarization, of the relative phase, or both. However, this description of the channel does not take into account the possibility of photon absorption or photon emission. In fact, for realistic channels, photon absorption is the dominant error, whereas the creation of photons in a particular given mode at optical frequency can be safely neglected. With this in mind, the best choice for encoding information in photons is to assign the state $|0\rangle$ to sending no photon, with the simple idea that, if one sends no photon, it cannot be absorbed. The state $|1\rangle$ is chosen as one of the polarization states. Therefore, this channel acts as follows

$$|0\rangle \mapsto |0\rangle T_0 \quad (2a)$$

$$|1\rangle \mapsto |1\rangle T_1 + |0\rangle T_a \quad (2b)$$

where we have omitted the initial state of the environment. The operator T_a describes the disappearance of a photon of the chosen polarization, due either to photon absorption or to a polarization change. We emphasize that this formulation of encoding and transmission (Eq. 2) incorporates more physical processes (that is, is more general) and yet is simpler than the one using two polarizations (see Eq. 1).

We must include in the description of the channel the fact that the photon is created by matter. In general, we can assume that the photon is produced by making an atom change its internal state. We wish to describe this process in the most general fashion. We consider two atoms A and B belonging to Alice and Bob, respectively. We denote by $|0\rangle$ and $|1\rangle$ two internal levels of the atoms, and by $|x\rangle$ any other level that may be involved in the process. As in (5), we consider a transmission process in which the sending atom will produce a photon only if it is in the state $|1\rangle$. Under ideal conditions, this photon will be absorbed by the receiving atom, which will be transferred from the state $|0\rangle \mapsto |1\rangle$. In reality, there will be errors involving both atoms and photons. For the photons, all possible errors are described by Eq. 2. For the atoms, we only require that if the sending atom is in the state $|0\rangle$, then no photon is produced; and if no photon reaches the receiving atom, which is in the state $|0\rangle$, it does not change state. Any other error can take place; for example, transfer of the atom to any other state $|x\rangle$. In order to keep the atoms in the 2D Hilbert space after the transmission, we optically pump the sending atom to the state $|0\rangle$; and in the receiving atom, we pump any state $|x \neq 0, 1\rangle$ to the state $|0\rangle$ (9). The states of the atoms undergo the following process:

$$|0\rangle_A|0\rangle_B \mapsto |0\rangle_A|0\rangle_B T_0 \quad (3a)$$

$$|1\rangle_A|0\rangle_B \mapsto |0\rangle_A(|1\rangle_B T_1 + |0\rangle_B T_a) \quad (3b)$$

T_0, T_1, and T_a contain spontaneous emission errors, photon absorption, and transitions to other states, followed by repumping to $|0\rangle$; all the physics is in these formulas. A possible way of implementing the process described by Eq. 3 is to use the scheme of (5). In a quantum network, there might be other atoms entangled with A and B. We emphasize that the above definition also applies to this situation. In the following, we will call a channel defined by Eq. 3 the photonic channel. The goal is thus to establish a perfect EPR pair, using the photonic channel. It is instructive to consider the channel as defined in Eq. 3, using its classical definition. There are nonzero probabilities of errors described by the operators σ_z and $\sigma_- = (\sigma_x - i\sigma_y)/2$. Straightforward application of the standard purification scheme to a situation with a finite number of atoms is not possible.

The possibility of (error-free) local quantum computing allows us to reduce the photonic channel (Eq. 3) to a channel without the absorptive term T_a. We will first present an outline of the key idea and then describe the process in detail. Let us assume that Alice has an initial arbitrary state in atom A (which could be entangled with other atoms in the network). Bob has atom B initially in state $|0\rangle_B$. In addition, Alice and Bob need two and one auxiliary atoms in state $|0\rangle$, respectively. Alice performs local operations with her particles and makes several transmissions to Bob using the photonic channel. Bob performs local operations and measurements. For a positive outcome of the measurement (see below), the mapping between the initial and the final state is given by

$$|0\rangle_A|0\rangle_B \mapsto |0\rangle_A|0\rangle_B S_0 \quad (4a)$$

$$|1\rangle_A|0\rangle_B \mapsto |1\rangle_A|1\rangle_B S_1 \quad (4b)$$

where the operators S act on the environment (see below for the specific form), and the auxiliary atoms end up in $|0\rangle$. For the opposite outcome, we recover the initial state of all atoms perfectly. By repeat-

ing the above scheme until a positive outcome is obtained, one accomplishes the mapping of Eq. 4 with certainty. The above protocol defines an "effective channel" that is absorption free: By comparing Eq. 3 with Eq. 4 we see that the effective channel acts like the photonic channel but without an absorption term (T_a). In the following, we will call channel reduction a protocol that combines local quantum computing with several transmissions to obtain an effective, less noisy channel.

The proof of the channel reduction involves two layers of protocols, which we describe here. (i) Alice applies a controlled-NOT operation to atom A and an auxiliary atom, and then uses the photonic channel to transmit the state of this atom to B. The mapping of this protocol will be

$$|0\rangle_A|0\rangle_B \mapsto |0\rangle_A|0\rangle_B T_0 \quad (5a)$$

$$|1\rangle_A|0\rangle_B \mapsto |1\rangle_A|1\rangle_B T_1 + |1\rangle_A|0\rangle_B T_a \quad (5b)$$

where the state of the auxiliary atom factorizes out. Equation 5 corresponds to an effective channel, which will be used in the following. (ii) We apply a Hadamard transformation to atom A, followed by a controlled-NOT with the auxiliary atom A_1 (which acts as a backup). Then we transmit the qubit A to B (at time t) according to Eq. 5, apply the operation NOT to atom A, transmit the qubit A to B_1 (at time t') according to Eq. 5, and apply a NOT operation to atom A again. Now a measurement is performed on atoms B and B_1 to check whether they are in the state $|0\rangle_B|0\rangle_{B_1}$: (a) If the outcome is "no," we perform the unitary transformation $|0\rangle_B|1\rangle_{B_1} \mapsto |0\rangle_B|0\rangle_{B_1}$, and $|1\rangle_B|0\rangle_{B_1} \mapsto |1\rangle_B|0\rangle_{B_1}$, and measure the state of A_2. If the outcome is $|0\rangle_{A_2}$, then we have Eq. 4 with $S_0 = T_1(t')T_0(t)$ and $S_1 = T_0(t')T_1(t)$, and similarly if $|1\rangle_{A_2}$. Here $T_{0,1}(t)$ and $T_{0,1}(t')$ denote the environment operators acting at time t and t' (first and second transmission, respectively). (b) If the outcome is "yes," we measure the state of A and then swap the state of A_1 into A. If the outcome was $|0\rangle_A$, then one has

$$|0\rangle_A|0\rangle_B \mapsto |0\rangle_A|0\rangle_B S_a \quad (6a)$$

$$|1\rangle_A|0\rangle_B \mapsto |1\rangle_A|0\rangle_B S_a \quad (6b)$$

with $S_a = T_a(t')T_0(t)$, and similarly if it is $|1\rangle_A$. This mapping is the identity, because the environment operator factors out. Therefore, we can repeat this protocol until we obtain a "no" in the measurement.

We define a stationary channel as the one fulfilling

$$T_1(t')T_0(t) = T_0(t')T_1(t) \quad (7)$$

when acting on the environment. In particular, this is true if the Markovian property considered in our previous work (6) holds. In that work, photon absorption was modeled with a Markovian master equation, and the other errors were assumed to be systematic (that is, the same in two subsequent transmissions). In the stationary limit (Eq. 7), the channel in Eq. 4 allows for ideal transmission in a single try. In contrast, we are interested in the general case where the stationarity property does not apply. In particular, this will be the case where there are additional random errors and when a Markovian description of decoherence is questionable. In the following, we will show how to establish distant EPR pairs using the channel in Eq. 4.

Alice and Bob repeatedly perform the process described below. In the Nth intermediate stage, the state of particles A and B is a superposition of two Bell states ("right" and "wrong") $|R\rangle_{AB} = |0\rangle_A|0\rangle_B + |1\rangle_A|1\rangle_B$ and $|W\rangle_{AB} = |0\rangle_A|1\rangle_B + |1\rangle_A|0\rangle_B$ (we omit normalization factors of $1/\sqrt{2}$)

$$|\Psi^{(N)}\rangle = |R\rangle_{AB}|E_R^{(N)}\rangle + |W\rangle_{AB}|E_W^{(N)}\rangle \quad (8)$$

where $|E_{R,W}^{(N)}\rangle$ are unnormalized states of the environment. In order to characterize the quality of the state in Eq. 8, we define its fidelity as $F_N = \||E_R^{(N)}\rangle\|^2$. The goal is to increase the fidelity so that for large N the state of the system will tend to $|R\rangle$.

Initially, Alice prepares her qubit A in the state $|+\rangle_A$ and Bob prepares his qubit B in $|0\rangle_B$. They use the channel in Eq. 4, and then both of them apply the local Hadamard operation $|0\rangle \mapsto |+\rangle$, and $|1\rangle \mapsto |-\rangle$, where we have defined $|\pm\rangle = |0\rangle \pm |1\rangle$. They obtain Eq. 8 with $|E^1_{R,W}\rangle = 1/2(S_0 \pm S_1)|E\rangle$, where $|E\rangle$ is the initial state of the environment. They repeatedly perform the following process using two auxiliary atoms A_2 and B_2.

1) The auxiliary qubit A_2 is locally entangled with the qubit A according to the transformation $|0\rangle_A|0\rangle_{A_2} \mapsto |0\rangle_A|+\rangle_{A_2}$, and $|1\rangle_A|0\rangle_{A_2} \mapsto |1\rangle_A|-\rangle_{A_2}$.

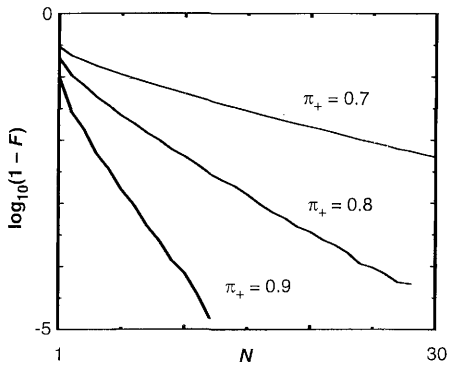

Fig. 1. Plot of the logarithm of the mean value of $1 - F_N$ as function of the number of steps N for $\pi_+ = 0.9$, 0.8, and 0.7.

2) The qubit A_2 is transmitted to the auxiliary qubit B_2 according to the effective channel of Eq. 4. Then the qubit A_2 is measured in the $|\pm\rangle_{A_2}$ basis. If the result is $|-\rangle_{A_2}$, one applies the unitary operation $|1\rangle_{B_2} \mapsto -|1\rangle_{B_2}$. Then one applies the transformation $|1\rangle_B|1\rangle_{B_2} \mapsto -|1\rangle_B|1\rangle_{B_2}$. The state after the transmission will be

$$|\Phi^{(N)}\rangle = |R\rangle_{AB}(|0\rangle_{B_2}S_0 + |1\rangle_{B_2}S_1)|E_R^{(N)}\rangle + |W\rangle_{AB}(|0\rangle_{B_2}S_0 - |1\rangle_{B_2}S_1)|E_W^{(N)}\rangle \quad (9)$$

3) The auxiliary qubit B_2 is measured. If the outcome is $|\pm\rangle_{B_2}$, the state becomes Eq. 8 with

$$|E_{R,W}^{(N+1)}\rangle = \frac{1}{2}(S_0 \pm S_1)|E_{R,W}^{(N)}\rangle \quad (10a)$$

$$|E_{R,W}^{(N+1)}\rangle = \frac{1}{2}(S_0 \mp S_1)|E_{R,W}^{(N)}\rangle \quad (10b)$$

respectively. We will denote the probability of these outcomes by $P_\pm$.

We analyze how the fidelity changes after each step, for which we need to evaluate $P_\pm$. To this end we define

$$\pi_\pm \equiv \frac{\left\|\frac{1}{2}(S_0 \pm S_1)|E\rangle\right\|^2}{\||E\rangle\|^2} \quad (11)$$

This parameter gives the probability that, starting from a perfect EPR pair, after one step we obtain the outcome $|\pm\rangle_{B_2}$. To calculate $\pi_\pm$, one needs to know the specific form of the operators and states at all times. We will estimate the change in the fidelity by assuming that $\pi_\pm$ does not depend on $|E\rangle$. Using the definition of Eq. 11, we have $P_\pm = \pi_\pm F_N + \pi_\mp(1 - F_N)$. Then, depending on the outcome of the measurement $|\pm\rangle_{B_2}$ the new fidelity is

$$F_{N+1} = \frac{\pi_\pm F_N}{\pi_\pm F_N + \pi_\mp(1 - F_N)} \quad (12)$$

respectively. For $\pi_+ > \pi_-$, the outcome $|+\rangle_{B_2}$ increases the fidelity and occurs with a higher probability. Because the decrease in fidelity after a $|-\rangle_{B_2}$ measurement is compensated for by a subsequent $|+\rangle_{B_2}$ measurement, the protocol consists of a random walk along a set of particular values of F, where it is more likely to go up than to go down, thus achieving $F \uparrow 1$ asymptotically. The process depends only on the value of π_+, which characterizes the effective channel; a good channel has a $\pi_+ \simeq 1$ (for the stationary channel, $\pi_+ = 1$).

We have simulated the improvement of the fidelity for several values of the probability π_+. In Fig. 1, we have plotted the logarithm of the mean value of $1 - F_N$ as a function of the number of steps N for π_+

= 0.9, 0.8, and 0.7. For example, we obtain $F = 1 - 10^{-5}$ after $N = 12$ steps for $\pi_+ = 0.9$. For general channels the fidelity approaches $F \sim 1 - e^{-cN}$, with N the number of steps. We emphasize that for $\pi_+ = 1$ we have a stationary channel. In this case, we obtain $F_1 = 1$ in a single step.

For a "good" standard channel (see Eq. 3), T_0 is close to T_1. As a consequence of our reduction procedure, this implies that $S_0 \simeq S_1$ and therefore $\pi_+ \simeq 1$, and $\pi_- \ll 1$. We emphasize that the reverse statement is not true; namely, one can have $S_0 \simeq S_1$ but a "bad" standard channel. Consider, for example, a very simple toy model in which the environment is a qubit in the initial state $|0\rangle$, and with $T_0 = \mathbb{1}$ and $T_1 = \sigma_x$. With the classical definition of a channel, one can easily show that this channel cannot produce entanglement; suppose that Alice has an entangled state of two qubits A and A_2, $|\alpha\rangle_A|0\rangle_{A_2} + |\beta\rangle_A|1\rangle_{A_2}$, and sends the second qubit to the qubit B of Bob via such a channel. The state after this transmission will be a mixed state $|\alpha\rangle_A\langle\alpha||0\rangle_B\langle 0| + \langle\beta\rangle_A\langle\beta||1\rangle_B\langle 1|$ and therefore is not entangled. However, for this channel $S_0 = S_1 = \sigma_x$, and therefore one can establish an EPR pair with the procedure introduced above. By twice using the channel as we proposed, the state of the environment after both transmission factorizes out, and therefore entanglement can be produced. When $S_0 \simeq S_1$, then $\pi_- \propto \|(S_0 - S_1)|E\rangle\|^2 \simeq 0$, which is due to quantum interference between the first and second transmission, using the reduction scheme of Eq. 4.

We have defined a photonic channel where $|0\rangle$ is assigned to sending no photon and $|1\rangle$ is assigned to sending one photon. Using local quantum computing with three and two auxiliary atoms in the first and second node, we have reduced it to an absorption-free channel. We have proposed a scheme based on this channel that iteratively improves the fidelity of distant EPR pairs, using quantum interference between two transmissions. For a stationary channel, one obtains a pure EPR pair in a single step. For a general channel, the fidelity approaches 1 exponentially with the number of steps.

REFERENCES AND NOTES

1. W. K. Wootters and W. H. Zurek, *Nature* **299**, 802 (1982).
2. C. H. Bennett, *Phys. Today* **48** (no. 1), 24 (1995).
3. C. H. Bennett *et al.*, *Phys. Rev. Lett.* **76**, 722 (1996); A. Ekert and C. Macchiavello, *ibid.* **77**, 2585 (1996).
4. P. W. Shor, *Phys. Rev. A* **52**, 2493 (1995); A. M. Steane, *Phys. Rev. Lett.* **77**, 793 (1996); E. Knill and R. Laflamme, *Phys. Rev. A* **55**, 900 (1997); J. I. Cirac, T. Pellizzari, P. Zoller, *Science* **273**, 1207 (1996).
5. J. I. Cirac, P. Zoller, H. Mabuchi, H. J. Kimble, *Phys. Rev. Lett.* **78**, 3221 (1997).
6. S. J. van Enk, J. I. Cirac, P. Zoller, *Phys. Rev. Lett.* **78**, 4293 (1997).
7. See, for example, B. Schumacher, *Phys. Rev. A* **45**, 2614 (1996); C. H. Bennett, D. P. DiVincenzo, J. A. Smolin, *Phys. Rev. Lett.* **78**, 3217 (1997).
8. C. H. Bennett *et al.*, *Phys. Rev. Lett.* **70**, 1895 (1993).
9. One can also use repumping techniques to supply fresh ancillas in error correction and purification. However, one still needs an infinite number to correct all errors.

10. This work was supported in part by the TMR network ERB-FMRX-CT96-0087 and by the Austrian Science Foundation.

2 July 1997; accepted 12 November 1997

A Laser Ablation Method for the Synthesis of Crystalline Semiconductor Nanowires

Alfredo M. Morales and Charles M. Lieber*

A method combining laser ablation cluster formation and vapor-liquid-solid (VLS) growth was developed for the synthesis of semiconductor nanowires. In this process, laser ablation was used to prepare nanometer-diameter catalyst clusters that define the size of wires produced by VLS growth. This approach was used to prepare bulk quantities of uniform single-crystal silicon and germanium nanowires with diameters of 6 to 20 and 3 to 9 nanometers, respectively, and lengths ranging from 1 to 30 micrometers. Studies carried out with different conditions and catalyst materials confirmed the central details of the growth mechanism and suggest that well-established phase diagrams can be used to predict rationally catalyst materials and growth conditions for the preparation of nanowires.

One-dimensional (1D) structures with nanometer diameters, such as nanotubes and nanowires, have great potential for testing and understanding fundamental concepts about the roles of dimensionality and size in, for example, optical, electrical, and mechanical properties and for applications ranging from probe microscopy tips to interconnections in nanoelectronics (*1*). The synthesis of crystalline semiconductor nanowires, such as Si and Ge (*2*), holds considerable technological promise for device applications and for improving the optical properties of these indirect gap materials but has been difficult to achieve. Several successful routes for the synthesis of carbon nanotubes are known (*3*), but the different bonding arrangement within these nanotubes and the different chemistry of carbon compared with Si and Ge would require an alternative approach for controlling the formation of nanowires from gas-phase reactants. Template-mediated methods that use zeolites, membranes, or nanotubes (*4*) can control growth but usually form polycrystalline materials.

An approach that does form crystalline wirelike structures is VLS growth (*5*, *6*), in which a liquid metal cluster or catalyst acts as the energetically favored site for absorption of gas-phase reactants. The cluster supersaturates and grows a 1D structure of the material; the lower limit of the diameter is generally >0.1 μm and is limited by the minimum diameter of the liquid metal catalysts that can be achieved under equilibrium conditions (*6*). A VLS method has been used to grow Si nanowires by confinement of Au metal on a surface (*7*, *8*), although the smallest diameters (20 to 100 nm) of defect-free nanowires are still relatively large. Recently, Buhro and co-workers have reported a promising solution-liquid-solid (SLS) synthesis of 10- to 100-nm-diameter III-V semiconductors (*9*). A potential limitation of the SLS approach, however, is the requirement of a catalyst that melts below the solvent boiling point.

We report an approach to the synthesis of single-crystal nanowires that exploits laser ablation to prepare nanometer-diameter catalyst clusters that subsequently define the size of wires produced by a VLS mechanism. This approach to generating nanometer-diameter clusters is understood from previous studies (*10*, *11*), and it overcomes the limitation of equilibrium cluster sizes in determining minimum wire diameters. We demonstrated this method with the synthesis of single-crystal Si and Ge nanowires with diameters as small as 6 and 3 nm, respectively, and lengths >1 μm. Because equilibrium phase diagrams can be used to rationally choose catalyst materials and growth conditions (*6*) and laser ablation can be used to generate nanometer-sized clusters of virtually any material, we believe that our approach could be adapted for preparing nanowires of numerous materials.

A. M. Morales, Department of Chemistry and Chemical Biology, Harvard University, Cambridge, MA 02138, USA.
C. M. Lieber, Department of Chemistry and Chemical Biology, and Division of Engineering and Applied Sciences, Harvard University, Cambridge, MA 02138, USA.

*To whom correspondence should be addressed. E-mail: cml@cmliris.harvard.edu